

ORIGINAL RESEARCH

Cochlear nerve visualization in Normal anatomy and inner ear malformations

Majed Assiri MD¹  | Tawfiq Khurayzi MD² | Fida Almuhawwas MD³ |
Kurt Schlemmer MD^{4,5,6} | Abdulrahman Hagr MD³ | Anandhan Dhanasingh PhD^{7,8} 

¹Abha Pediatric Hospital, Cochlear Implant Centre, Ministry of Health, Abha, Saudi Arabia

²King Fahad Central Hospital, Jizan, Saudi Arabia

³King Abdullah Ear Specialist Centre, King Saud University Medical City, King Saud University, Riyadh, Saudi Arabia

⁴Department of Speech-Language Pathology and Audiology, University of Pretoria, Pretoria, South Africa

⁵University of Kwazulu, Durban, South Africa

⁶Natal Department of Otorhinolaryngology-Head and Neck Surgery, Hillcrest Hospital, Durban, South Africa

⁷MED-EL Medical Electronics GmbH, Innsbruck, Austria

⁸Department of Translational Neurosciences, Faculty of Medicine and Health Sciences, University of Antwerp, Antwerp, Belgium

Correspondence

Majed Assiri, Abha Pediatric Hospital, Cochlear Implant Centre, Ministry of Health, Abha, Saudi Arabia.

Email: majedeisa@gmail.com

Abstract

Objectives: This study aimed to qualitatively evaluate the variations in nerve bundles between patients with normal anatomy and those with inner-ear anomalies.

Methods: Magnetic resonance imaging (MRI) scans of the temporal bones of candidates for cochlear implants (CIs) enrolled at a tertiary center were retrospectively reviewed from the clinical database. The 3.0-Tesla MRI scans were analyzed using a three-dimensional slicer to visualize the nerve bundles in the internal auditory canal.

Results: A total of 49 ears were analyzed. Twenty ears exhibited normal inner ear anatomy, whereas 29 ears had various inner-ear malformations. The cochlear nerve (CN) was visible on all 20 scans with normal inner-ear anatomy. In addition, the CN was visualized in 18 scans with inner ear malformations. Furthermore, the CN was identified in six of the eight scans with IP type I, whereas in two scans, the CN and vestibular nerve were unclear. Three scans with a common cavity showed only two nerve bundles.

Conclusion: The findings of this study show that the CN can be visualized in most inner-ear anatomical types. Even in severely malformed inner ears, the common nerve bundle that represents the cochlear and vestibular nerves can be visualized. The MRI is highly recommended for CN assessment before CI surgery.

Level of Evidence: Level IV.

KEYWORDS

cochlea, cochlear implant, cochlear nerve, inner ear, MRI

1 | INTRODUCTION

The World Health Organization (WHO) reports more than 430 million individuals are suffering with disabling hearing loss.¹ Although hearing aids represent a straightforward solution for amplifying sound in those experiencing disabling hearing loss, they may fall short in delivering adequate benefits for certain individuals dealing with severe

sensorineural hearing loss (SNHL).² Cochlear implants (CIs) have emerged as the golden standard in restoring hearing functionality among individuals with SNHL.^{3,4} Cochlear implant provides electrical stimulation from the intracochlear electrode array. This stimulation is then detected by the neural elements residing within the cochlea, subsequently traversing the cochlear nerve (CN) situated in the internal auditory canal (IAC). It further goes through the higher-level auditory

This is an open access article under the terms of the [Creative Commons Attribution-NonCommercial-NoDerivs](https://creativecommons.org/licenses/by-nc-nd/4.0/) License, which permits use and distribution in any medium, provided the original work is properly cited, the use is non-commercial and no modifications or adaptations are made.

© 2024 The Author(s). *Laryngoscope Investigative Otolaryngology* published by Wiley Periodicals LLC on behalf of The Triological Society.

pathway until it reaches the auditory cortex, resulting in the perception of sound by the recipient.^{5,6}

Given the pivotal role played by the CN in determining the success of cochlear implant outcomes, it is of vital importance to subject it to thorough preoperative evaluation. Nerves and soft tissues are better visualized using magnetic resonance imaging (MRI) than computed tomography (CT) images.^{7,8} The presence of the CN in the IAC increases the probability of effective CI therapy.⁹ The cross section at the mid-length of the IAC in a normal anatomy inner ear shows four nerve bundles, including one from the CN, two from the vestibular nerve (VN), and one from the facial nerve (FN).^{10,11}

As per literature reports, 20%–30% of congenital hearing loss subjects have some degrees of inner-ear malformations (IEM).¹² The success of CIs in IEM cases depends on the severity of malformation seen in the cochlear portion and in the presence of CN.^{13,14} Despite the clinical significance of this relationship, a noticeable gap exists in the literature regarding reports on the presence of the cochlear nerve (CN) across all types of inner-ear malformations.¹⁵

To address this knowledge gap, the present study is designed to examine the cross-sectional anatomy of IAC across various types of inner-ear anatomical types, leveraging advanced magnetic resonance imaging (MRI) techniques. The primary objective is to provide a

qualitative analysis on the presence of CN between ears identified with normal anatomy and those afflicted with various forms of IEMs.

2 | MATERIALS AND METHODS

2.1 | Image selection

The clinical database of our center was retrospectively searched for MRI scans of the temporal bones of CI candidates enrolled between 2011 and 2022. The Institutional Review Board approved (No.: E-21-5737) the use of images in this study after anonymization. MRI of the temporal bone was performed using a 3.0-Tesla scanner (GE Discovery 750 HD; General Electric Company, Waukesha, WI, USA). The settings for T2-weighted fast imaging were as follows: steady-state acquisition (FIESTA) frequency matrix, 320; phase matrix, 256; number of averages, 2; slice thickness, 1.0–0.6 mm; overlap, 0.3; flip angle, 358; field of view, 18; phase field of view, 0.75; frequency matrix, 320; and phase matrix, 256. The MRI scans were analyzed using a three-dimensional (3D) slicer freeware, version 4.11.202110226 (<https://www.slicer.org>).

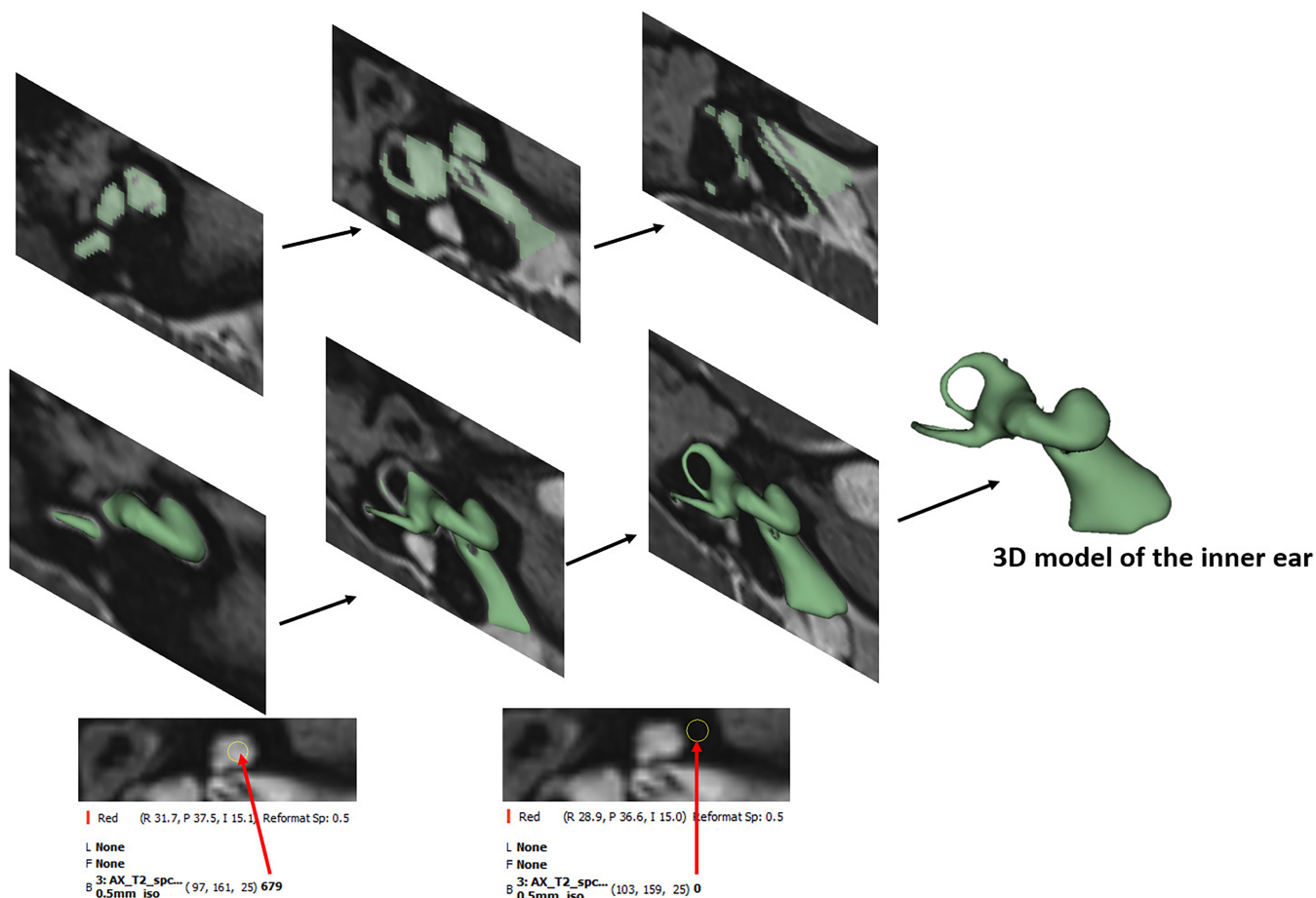


FIGURE 1 3D reconstruction of magnetic resonance images of the inner ear. Reconstruction was performed by manually selecting image slices showing the inner ear structures by setting a tight grayscale threshold.

2.2 | Image analyses

Three-dimensional reconstruction of the inner ear was performed as described previously by Dhanasingh et al.¹⁶ Briefly, the inner ear structures were captured by setting tight grayscale thresholds for the fluid-filled region. Figure 1 shows an example of grayscale thresholding. The greyscale of the otic capsule is 0 (dark = bone in MRI), whereas that of the membranous labyrinth is 679 (bright = fluid in MRI); thus, the lower threshold for this sample was set as 679. The mid-length cross section of the IAC in the oblique sagittal view can be used to visualize the nerve bundles, as shown in Figure 2A. Figure 2B shows the corresponding IAC cross section showing four distinct nerve bundles. Video S1 file visually demonstrates the steps involved in 3D segmentation of the inner ear and c/s of IAC to visualize CN.

2.3 | Classification of anatomical types

We followed Sennaroglu's inner ear classification method to differentiate each of the anatomical types.¹⁷ Briefly, a normal anatomy (NA) inner ear shows the presence of different turns of the cochlea along with the clear distinction of three semicircular canals. Enlarged vestibular aqueduct syndrome (EVAS) shows enlarged vestibular aqueduct sac in addition to almost normal anatomy inner ear. Incomplete partition (IP) type II shows normal development of basal turn of the cochlea to around 180° of angular depth beyond with the cochlea appears cystic along with enlarged vestibular aqueduct sac. IP type I is more severely malformed with cochlear portion completely cystic separated from the vestibular portion. IP III is characterized by complete absence of mid modiolar trunk, cochlear turns too tightly toward the apex and wide IAC, all result of genetic disorder. Cochlear hypoplasia (CH) refers to underdeveloped cochlea associated with smaller sized not fully developed inner ear structures. Vestibular cavity (VC) represents a cavity that belongs to the vestibular portion with a clear absence of the cochlear portion, whereas common cavity

(CC) represents a cavity that is common for both cochlear and vestibular portion. Figure 3 shows 3D-segmented inner ear of all anatomical types taken for analysis in this study.

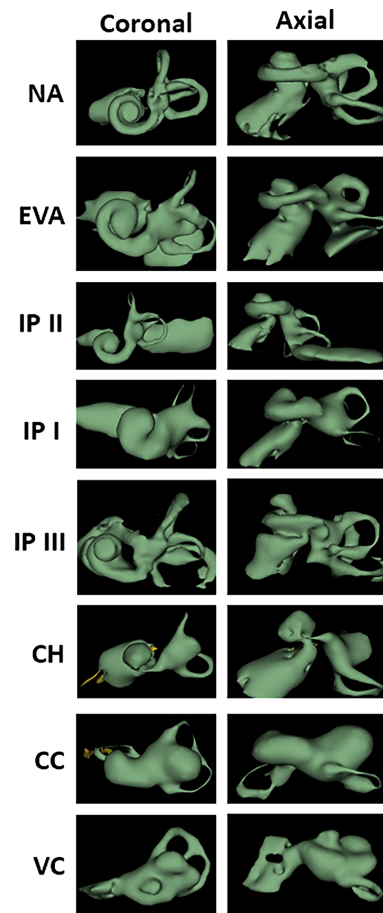


FIGURE 3 3D reconstruction of inner ear of all anatomical types taken for analysis are shown in both coronal and axial view.

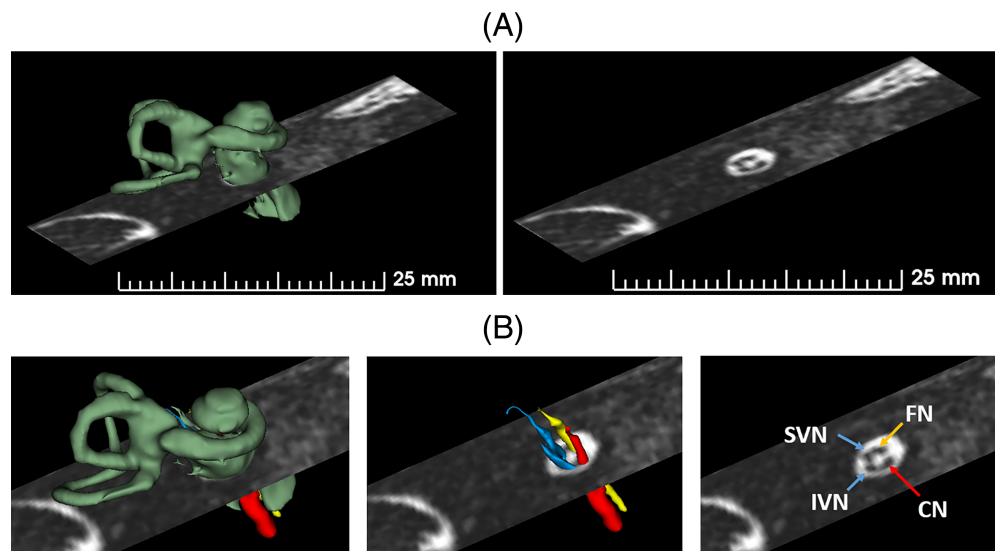


FIGURE 2 3D reconstruction of an inner ear with normal anatomy with the image slice cutting through the mid-length of the IAC (A). IAC cross section showing four distinct nerve bundles (B).

TABLE 1 Anatomical types of the inner ear identified, and the number of scans shows the presence of CN.

S. No	Anatomical types	Number of Scans	Number of scans showing CN presence
1	Normal anatomy	20	20 (100%)
2	Enlarged vestibular aqueduct syndrome	5	5 (100%)
3	Incomplete partition type I	8	5 (62.5%)
4	Incomplete partition type II	4	3 (75%)
5	Incomplete partition type III	4	4 (100%)
6	Cochlear hypoplasia	4	3 (75%)
7	Vestibular cavity	3	0 (0%)
8	Classic common cavity	1	0 (0%)
Total		49	40 (81.6%)

3 | RESULTS

3.1 | Demographics

Table 1 includes the different inner-ear anatomical types identified and the number of ears evaluated per anatomical type. Age and sex data were not available because of the data protection policies of our center. A total of 49 ears from 49 subjects were analyzed either taking right or left side randomly.

3.2 | Number of nerve bundles

In patients with normal inner-ear anatomy, the IAC cross section showed four distinct nerve bundles representing the FN, CN, superior VN, and inferior VN as shown in Figure 3.

Figure 4 shows the IAC cross section for all 49 datasets analyzed. The CN as pointed by yellow arrow can be identified in all 20 scans (1–20) with normal inner-ear anatomy, and two scans marked with * show the VN displaced toward the edge of the IAC. All four nerve bundles can be identified in all five scans (21–25) with EVAS. The CN can be identified in all four scans (26–29) with IP II, but two scans (28 and 29) marked with * show some deformity in the VN alone. The CN can be identified in five (30–32; 35, 36) out of eight scans (30–37) with IP I, whereas the CN and VN are not conclusively identified on scans 33, 34 and 37 as marked with *. All nerve bundles are identified in four scans (38–41) of IP III. Among the four scans (42–45) with CH, all four nerve bundles can be identified on three scans (43–45), whereas the VN is not conclusively identified on one scan (42) marked with *. All three scans with vestibular cavities (VCs) and one with classic CC scan show only two nerve bundles.

3.3 | Cross-sectional shape of the IAC

Qualitative evaluation of the images in Figure 4 showed that the cross-sectional shape of the IAC was not round but rather distorted.

In addition, the position of the nerve bundles in the IAC cross section was not uniform in all cases analyzed. The superior and inferior VNs were seen separately in most scans with normal inner-ear anatomy, whereas they were seen as a combined single nerve bundle with an elliptical shape in ears with EVAS; IP types I, II, and III; and CH. All scans with VC and CC showed an elliptical IAC cross section.

4 | DISCUSSION

Previous studies have reported visualization of the CN in some anatomical types.^{18,19} To the best of our knowledge, this is the first study to demonstrate the CN in several samples of most of inner-ear anatomical types.

In this study, distinct nerve bundles were identified in most cases of all malformation types other than CC and VC. The cochlea and a portion of the CN have the same embryological origin (otic placode), and they potentially exhibit a similar developmental arrest.¹⁵ Around the fourth week of pregnancy, a group of neuroblasts from the otocyst delaminate and migrate between the developing inner ear and the hindbrain; these later differentiate into the CN and VN inside the IAC.^{20,21} Developmental arrest in the 4th week of gestation, which results in the CC and VC types of malformations, may lead to disturbance in the development of a distinct cochlear nerve, as observed in the four samples (three VC and one CC) analyzed in this study.

Visualizing the CN at the mid-length of the IAC on MRI is prognostic for a successful CI treatment. Talenti et al. reported on the presence of CN in CH and IP types I, II, and III in the axial view but not in the oblique sagittal view, which differs from the findings of our study.²² The CN is observed in all inner-ear anatomical types other than the CC and VC that have distinct cochlear development. This could explain the worse hearing outcomes with CI in the CC and VC types and better outcomes in the EVAS type in the study by Ozkan et al.²³

The CN was visualized in most of the samples in this study, regardless of the inner-ear anatomical types. Thus, it shows that the CN deficiency is not mainly associated with inner ear anatomical types

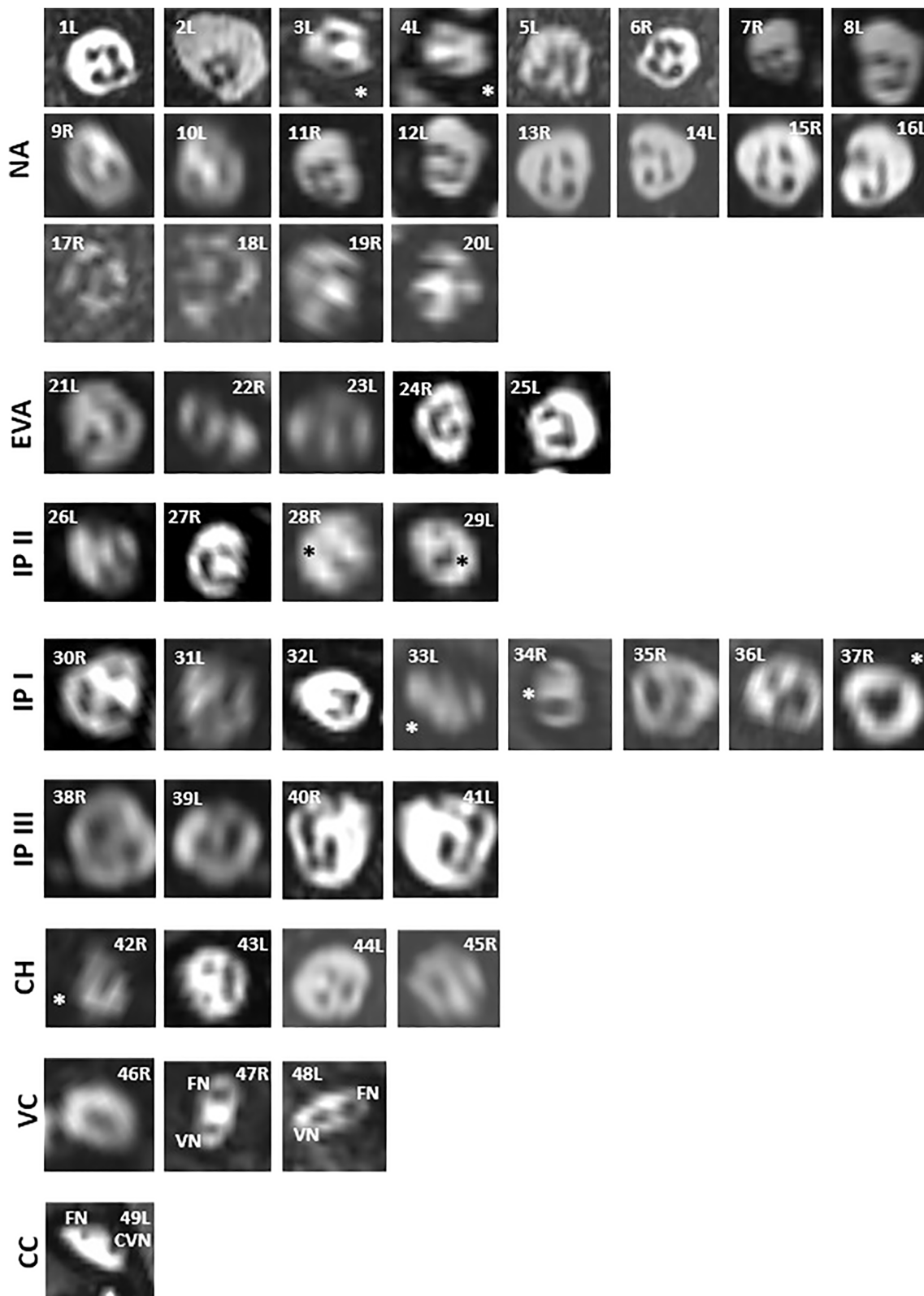


FIGURE 4 Mid-length cross sections of the IAC from all scans analyzed in this study showing the nerve bundles. R: Right side ear; L: Left side ear. The symbol * refers to cases identified with a deficiency in one of the nerve bundles.

and raises the awareness of using MRI in for individual analysis of every case with congenital deafness before CI surgery. Although MRI requires general anesthesia in children and is expensive, it is worth

the cost.^{24,25} The overall cross-sectional shape of the IAC and individual locations of the nerve bundles within the IAC varied considerably between the samples analyzed.

Study limitations include not standardizing the angle of the plane by which the IAC is cross-sectioned, and this affects the size and shape of every nerve bundle visualized. Also, some samples had slice thickness of 1 mm with which it is hard to define the boundary of CN to quantify the size in comparison to other nerve bundles. Although we had 49 MRI scans of the complete temporal bone in total, we looked at one side of the ear only assuming symmetry and choosing the side randomly. A large sample size or systematic review could help in understanding the correlation between inner-ear anomalies and CN anatomy in the IAC, which could facilitate preoperative counseling and appropriately match patients' expectations.

In our series, few samples within the IEM types like IP II, IP I, and CH showed either the absence or the doubtful presence of CN highlighting the clinical significance of routine preoperative checking for the presence of CN.

5 | CONCLUSIONS

The CN can be visualized in most inner-ear anatomical types. Even the most severe malformations, such as CC and VC with cochlear aplasia, show a common nerve bundle that represents the cochlear and vestibular nerves. MRI is highly recommended to visualize the CN before CI surgery in patients with congenital deafness.

ACKNOWLEDGMENTS

The authors have nothing to acknowledge.

FUNDING INFORMATION

This research received no external funding.

CONFLICT OF INTEREST STATEMENT

Anandhan Dhanasingh is employed by MED-EL as the Head of Electrodes Research & Inner Ear Malformations within R&D department. The remaining authors declare no conflict of interest.

DATA AVAILABILITY STATEMENT

The data presented in this study are available from the corresponding author upon request.

INFORMED CONSENT STATEMENT

Patient consent was waived as all data were anonymized and reviewed retrospectively.

ORCID

Majed Assiri  <https://orcid.org/0000-0002-8733-2125>

Anandhan Dhanasingh  <https://orcid.org/0000-0003-2116-9318>

REFERENCES

- Deafness and Hearing Loss. Accessed 17 July 17, 2023. https://www.who.int/health-topics/hearing-loss#tab=tab_1
- Choi JE, Kim J, Yoon SH, Hong SH, Moon IJ. A personal sound amplification product compared to a basic hearing aid for speech intelligibility in adults with mild-to-moderate sensorineural hearing loss. *J Audiol Otol*. 2020;24:91-98. doi:10.7874/JAO.2019.00367
- Van de Heyning P, Gavilán J, Godey B, et al. Worldwide variation in Cochlear implant candidacy. *J Int Adv Otol*. 2022;18:196-202. doi:10.5152/IAO.2022.21470
- Blebea CM, Ujvary LP, Necula V, et al. Current concepts and future trends in increasing the benefits of Cochlear implantation: A narrative review. *Medicina (Kaunas)*. 2022;58:747. doi:10.3390/MEDICINA58060747
- Dhanasingh A, Hochmair I. Signal processing & audio processors. *Acta Otolaryngol*. 2021;141:106-134. doi:10.1080/00016489.2021.1888504
- Deep NL, Dowling EM, Jethanamest D, Carlson ML. Cochlear implantation: an overview. *J Neurol Surg B Skull Base*. 2019;80:169-177. doi:10.1055/S-0038-1669411
- Chang AE, Matory YL, Dwyer AJ, et al. Magnetic resonance imaging versus computed tomography in the evaluation of soft tissue tumors of the extremities. *Ann Surg*. 1987;205:340-348. doi:10.1097/0000658-198704000-00002
- Valvassori GE, Palacios E. Magnetic resonance imaging of the internal auditory canal. *Top Magn Reson Imaging*. 2000;11:52-65. doi:10.1097/00002142-200002000-00007
- Han JJ, Suh MW, Park MK, Koo JW, Lee JH, Oh SH. A predictive model for Cochlear implant outcome in children with Cochlear nerve deficiency. *Sci Rep*. 2019;9:1154. doi:10.1038/S41598-018-37014-7
- Young JY, Ryan ME, Young NM. Preoperative imaging of sensorineural hearing loss in pediatric candidates for Cochlear implantation. *Radiographics*. 2014;34:E133-E149. doi:10.1148/RG.345130083
- Verstappen G, Foulon I, Van den Houte K, et al. Analysis of congenital hearing loss after neonatal hearing screening. *Front Pediatr*. 2023;11:1153123. doi:10.3389/FPED.2023.1153123
- Sennaroglu L, Saatci I. A new classification for cochleovestibular malformations. *Laryngoscope*. 2002;112:2230-2241. doi:10.1097/00005537-200212000-00019
- Farhood Z, Nguyen SA, Miller SC, Holcomb MA, Meyer TA, Rizk HG. Cochlear implantation in inner ear malformations: systematic review of speech perception outcomes and intraoperative findings. *Otolaryngol Head Neck Surg*. 2017;156:783-793. doi:10.1177/0194599817696502
- Degirmenci Uzun E, Batuk MO, D'Alessandro HD, Sennaroglu G. Auditory perception in pediatric Cochlear implant users with Cochlear nerve hypoplasia. *Int J Pediatr Otorhinolaryngol*. 2022;160:111248. doi:10.1016/J.IJPORL.2022.111248
- Dhanasingh A. The embryology of the Cochlear nerve and its radiological relevance. In: Li Y, ed. *Cochlear Implantation for Cochlear Nerve Deficiency*. Springer; 2022. doi:10.1007/978-981-19-5892-2_1
- Dhanasingh A, Dietz A, Jolly C, Roland P. Human inner-ear malformation types captured in 3D. *J Int Adv Otol*. 2019;15:77-82. doi:10.5152/IAO.2019.6246
- Sennaroglu L, Bajin MD. Classification and current management of inner ear malformations. *Balkan Med J*. 2017;34(5):397-411. doi:10.4274/balkanmedj.2017.0367
- Benson JC, Carlson ML, Lane JI. MRI of the internal auditory canal, labyrinth, and middle ear: how we do it. *Radiology*. 2020;297:252-265. doi:10.1148/RADIOL.2020201767
- Quirk B, Youssef A, Ganau M, D'Arco F. Radiological diagnosis of the inner ear malformations in children with sensorineural hearing loss. *BJR Open*. 2019;1(1):20180050. doi:10.1259/bjro.20180050
- Warnecke A, Giesemann A. Embryology, malformations, and rare diseases of the cochlea. *Laryngorhinootologie*. 2021;100:S1-S43. doi:10.1055/A-1349-3824
- Brotto D, Sorrentino F, Cenedese R, et al. Genetics of inner ear malformations: a review. *Audiol Res*. 2021;11:524-536. doi:10.3390/AUDIOLRES11040047
- Talenti G, Manara R, Brotto D, D'Arco F. High-resolution 3 T magnetic resonance findings in Cochlear hypoplasias and incomplete partition

- anomalies: a pictorial essay. *Br J Radiol*. 2018;91:20180120. doi:[10.1259/BJR.20180120](https://doi.org/10.1259/BJR.20180120)
23. Ozkan HB, Cicek Cinar B, Yucel E, Sennaroglu G, Sennaroglu L. Audiological performance in children with inner ear malformations before and after Cochlear implantation: a cohort study of 274 patients. *Clin Otolaryngol*. 2021;46:154-160. doi:[10.1111/COA.13625](https://doi.org/10.1111/COA.13625)
 24. Alzhrani F, Babkour A, Almuhawwas F, Sanosi A. Value of routine magnetic resonance imaging for the preoperative assessment of Cochlear implant candidates. *Cureus*. 2019;11:e6279. doi:[10.7759/CUREUS.6279](https://doi.org/10.7759/CUREUS.6279)
 25. Trimble K, Blaser S, James AL, Papsin BC. Computed tomography and/or magnetic resonance imaging before pediatric Cochlear implantation? Developing an investigative strategy. *Otol Neurotol*. 2007;28:317-324. doi:[10.1097/01.MAO.0000253285.40995.91](https://doi.org/10.1097/01.MAO.0000253285.40995.91)

SUPPORTING INFORMATION

Additional supporting information can be found online in the Supporting Information section at the end of this article.

How to cite this article: Assiri M, Khurayzi T, Almuhawwas F, Schlemmer K, Hagr A, Dhanasingh A. Cochlear nerve visualization in Normal anatomy and inner ear malformations. *Laryngoscope Investigative Otolaryngology*. 2024;9(6):e70023. doi:[10.1002/lio2.70023](https://doi.org/10.1002/lio2.70023)